

LA-UR-21-23824 (Accepted Manuscript)

# Application of saturation absorption spectroscopy to study the hyperfine structure of $^{235}\text{U}$ and accurate $^{235}\text{U}/^{238}\text{U}$ isotope ratio determinations at 861.031 nm

Wei, Wei  
Savukov, Igor Mykhaylovych  
Castro, Alonso

Provided by the author(s) and the Los Alamos National Laboratory (2021-08-04).

**To be published in:** Journal of Analytical Atomic Spectrometry

**DOI to publisher's version:** 10.1039/D1JA00140J

**Permalink to record:** <http://permalink.lanl.gov/object/view?what=info:lanl-repo/lareport/LA-UR-21-23824>

**Disclaimer:**

Los Alamos National Laboratory, an affirmative action/equal opportunity employer, is operated by Triad National Security, LLC for the National Nuclear Security Administration of U.S. Department of Energy under contract 89233218CNA000001. By approving this article, the publisher recognizes that the U.S. Government retains nonexclusive, royalty-free license to publish or reproduce the published form of this contribution, or to allow others to do so, for U.S. Government purposes. Los Alamos National Laboratory requests that the publisher identify this article as work performed under the auspices of the U.S. Department of Energy. Los Alamos National Laboratory strongly supports academic freedom and a researcher's right to publish; as an institution, however, the Laboratory does not endorse the viewpoint of a publication or guarantee its technical correctness.

# JAAS

Journal of Analytical Atomic Spectrometry

Accepted Manuscript

This article can be cited before page numbers have been issued, to do this please use: W. Wei, I. M. Savukov and A. Castro, *J. Anal. At. Spectrom.*, 2021, DOI: 10.1039/D1JA00140J.



This is an Accepted Manuscript, which has been through the Royal Society of Chemistry peer review process and has been accepted for publication.

Accepted Manuscripts are published online shortly after acceptance, before technical editing, formatting and proof reading. Using this free service, authors can make their results available to the community, in citable form, before we publish the edited article. We will replace this Accepted Manuscript with the edited and formatted Advance Article as soon as it is available.

You can find more information about Accepted Manuscripts in the [Information for Authors](#).

Please note that technical editing may introduce minor changes to the text and/or graphics, which may alter content. The journal's standard [Terms & Conditions](#) and the [Ethical guidelines](#) still apply. In no event shall the Royal Society of Chemistry be held responsible for any errors or omissions in this Accepted Manuscript or any consequences arising from the use of any information it contains.

# Application of saturation absorption spectroscopy to study the hyperfine structure of $^{235}\text{U}$ and accurate $^{235}\text{U}/^{238}\text{U}$ isotope ratio determinations at 861.031 nm

Wei Wei,<sup>a</sup> Igor Savukov,<sup>b</sup> and Alonso Castro<sup>a\*</sup>

## Abstract

The uranium transition  $5f^36d7s^2$  ( $^5\text{L}_6$ )  $\rightarrow$   $5f^37s^27p$  ( $^5\text{K}_5$ ) at 861.031 nm was studied using saturation absorption spectroscopy. The hyperfine structure of the  $^{235}\text{U}$  isotope was determined by measuring the Doppler-suppressed absorption spectrum, and the hyperfine structure constants were obtained by employing transition-specific line strength theory and spectral fitting. The magnetic-dipole and electric-quadrupole constants were determined to be  $A = -3.2887 \pm 0.1957$  mK and  $B = 31.8712 \pm 8.0789$  mK for the upper state  $5f^37s^27p$  ( $^5\text{K}_5$ ). A theoretical calculation for the hyperfine structure constants of the  $^{235}\text{U}$  isotope was also carried out by the relativistic configuration-interaction (RCI) method, and the obtained values were found to be in agreement with the measured values. In addition, the line profile of  $^{238}\text{U}$  was experimentally investigated for different excitation intensities and modeled using the RCI method for estimating the transition probability and oscillator strength, with various residual broadening mechanisms considered beyond the radiative decay. We show that these results allow us to make improvements on the precision of spectral measurements using our previously developed technique for isotope ratio determinations in atomic beams.

## Introduction

The isotopic analysis of uranium plays an important role in nuclear energy, nuclear forensics, and safeguards for nuclear non-proliferation<sup>1-3</sup>.  $^{235}\text{U}/^{238}\text{U}$  ratios are commonly used to differentiate between materials that contain natural or enriched uranium. Mass spectrometry is the most commonly used method for the isotopic analysis of the actinides, due to its high precision and sensitivity<sup>1</sup>. Mass spectrometry, however, requires extensive

<sup>a</sup>Chemistry Division and <sup>b</sup>Materials Physics and Applications Division, Los Alamos National Laboratory, Los Alamos, NM 87545, USA.

\*To whom correspondence should be addressed: acx@lanl.gov

sample preparation and chemical purification steps, because it is susceptible to isobaric interferences, i.e., when two isotopes of different elements having the same mass are present in the sample, and also polyatomic interferences, i.e., when the mass of a molecule matches that of an atom<sup>4</sup> (e.g., <sup>238</sup>U<sup>1</sup>H and <sup>239</sup>Pu). To overcome these challenges, we have developed methods and instrumentation for the isotopic analysis of the actinides by laser absorption spectroscopy in an atomic beam<sup>5-7</sup>. This method relies on the interaction between a collimated atomic beam, generated by a resistively-heated crucible, and a tunable narrow-linewidth laser in a saturation-spectroscopy configuration to reduce Doppler broadening. The isotopic composition of a uranium sample is determined from the ratio of the integrated absorption areas of <sup>235</sup>U and <sup>238</sup>U.

High-accuracy atomic absorption measurements depend on the knowledge of various spectral parameters for specific transitions, such as line center, line strength and line shape. <sup>235</sup>U exhibits a complex spectrum due to six optically active electrons (i.e., the 5f<sup>3</sup>6d7s<sup>2</sup> ground structure), and also hyperfine structure (hfs) due to its non-zero nuclear spin angular momentum. Gerstenkorn *et al.* conducted the first determination of hfs parameters of <sup>235</sup>U<sup>8</sup>. Childs *et al.* measured the hfs constants of the ground state and of the 620 cm<sup>-1</sup> metastable state<sup>9,10</sup>. Avril *et al.* reported an extensive study of the hfs constants for 28 low odd levels and 22 even levels<sup>11</sup>. Phillips *et al.* estimated the relative hyperfine line strengths for the 394.83 nm and 404.28 nm transitions<sup>12</sup>. These experiments are an important step towards the understanding of the atomic structure of uranium. However, further research is needed towards the elucidation of the structure of other energy levels, most notably, the 5f<sup>3</sup>7s<sup>2</sup>7p (<sup>5</sup>K<sub>5</sub>) level, which is involved in one of the strongest transitions of uranium at 861.031 nm (0 → 11613.977 cm<sup>-1</sup>), recently studied by Taylor *et al.*<sup>13</sup>.

In order to conduct high-precision measurements of the isotopic composition of uranium samples by absorption spectroscopy, it is necessary to minimize Doppler broadening, which can be accomplished in a collimated atomic beam. We have used resistively-heated tantalum foil micro-crucibles to generate atomic beams of uranium at temperatures up to 2600 °C<sup>6,7</sup>. At a typical working temperature of 2200 °C, the Boltzmann distribution,  $\exp(-\varepsilon/kT)$ , where  $\varepsilon$  is the state energy, roughly provides a relative

value of 1 for the ground state and 0.71 for the  $620\text{ cm}^{-1}$  metastable state. The next state above these two states has an energy of  $3800.8\text{ cm}^{-1}$  and  $\exp(-\varepsilon/kT)$  gives a value of 0.11, which is 9 times smaller than that of the ground state, and 6 times smaller than that of the first metastable state. With these relatively rough calculations, we conclude that at  $2200\text{ }^{\circ}\text{C}$  most of the neutral uranium atoms populate the ground and the first metastable states. Considering that the ground state has the largest population of uranium atoms, the transitions from the ground state are more suitable for sensitive spectroscopic techniques that utilize the absorption of laser light. Fig. 1 shows the relative emission line strengths of the strongest ground state transitions of uranium, according to Ref. 12. It can be seen that the strongest transition at  $861.031\text{ nm}$  is approximately 1.5 times stronger than the second strongest transition, which makes it suitable for high-precision absorption measurements at relatively low temperatures.

We have previously conducted absorption spectroscopy experiments in atomic beams for isotope ratio determinations at  $861.031\text{ nm}$ <sup>6,7</sup>, but the spectral parameters for this transition, especially the hfs of the upper energy state of  $^{235}\text{U}$  haven't been thoroughly studied yet. Separations of hyperfine transitions usually lie in the range from several wavenumbers to as little as hundredths of wavenumbers. Even with the use of collimated atomic beams to constrain the width of the transverse atomic velocity distribution, the resolution of hyperfine absorption spectroscopy can be still limited by any residual Doppler broadening caused by a divergence of the atomic beam, and also by other broadening mechanisms, including the finite lifetime of the levels, and self-collisional broadening. Consequently, hyperfine transitions cannot be fully resolved for some experimental arrangements, including incomplete collimation of the atomic beam due to the very small atomic fluxes obtained from low-vapor pressure elements, such as uranium. Saturation absorption spectroscopy (SAS), which can potentially eliminate Doppler broadening, has been utilized to obtain Doppler-free hyperfine spectra in the past<sup>15-17</sup>. Thus, to reduce the residual Doppler width from a divergent atomic beam, we have conducted SAS experiments on the  $11613.9771\text{ cm}^{-1}$  upper energy state involved in the  $861.031\text{ nm}$  transition of uranium, which, when combined with our theoretical calculations, can be of great value for uranium isotope ratio determinations. In addition, we have studied the linewidth broadening mechanisms of  $^{238}\text{U}$ , which is an important

parameter for implementing our spectroscopic technique. Ideally, the observed linewidth in saturation spectroscopy is expected to be dominated by the natural linewidth, but we found that other effects lead to substantially larger observed linewidths. Eliminating these effects in the future can lead to increased precision in the measurement of hyperfine parameters.

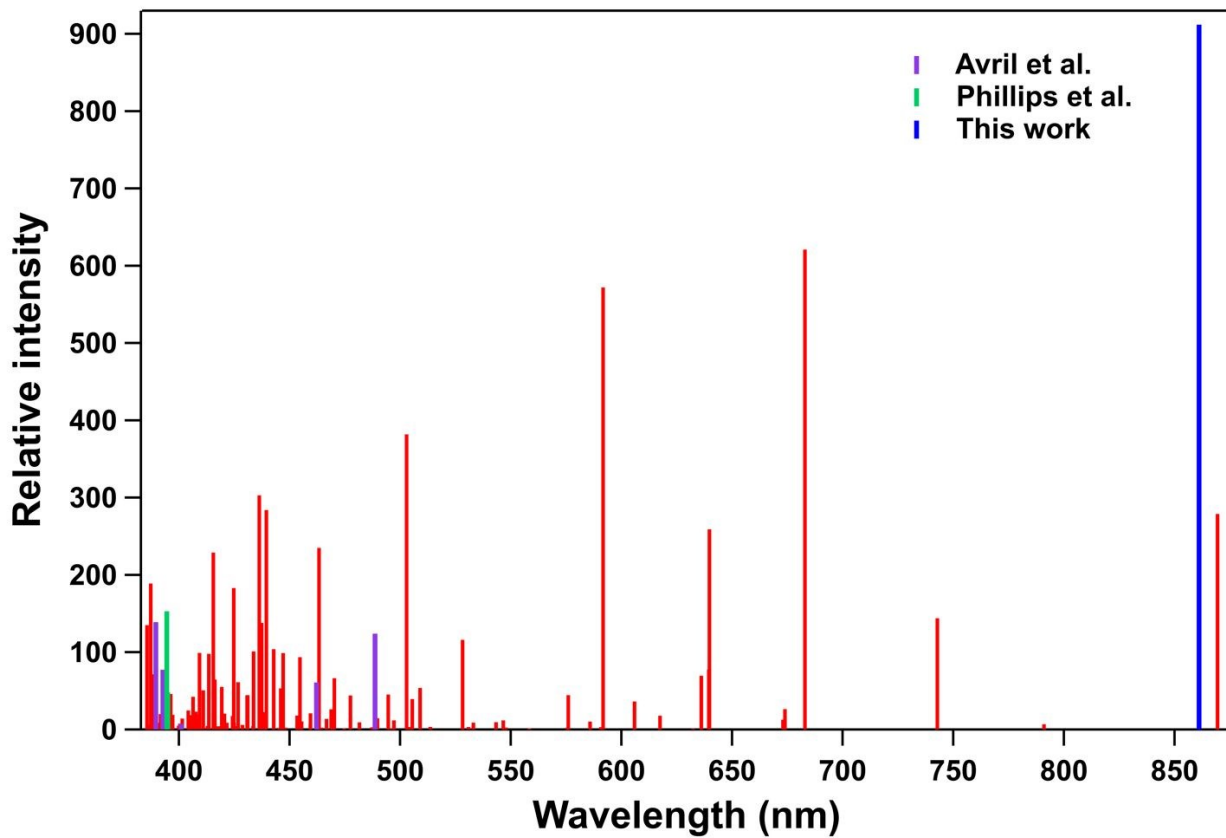


Fig. 1. Relative emission intensities of the strongest ground state transitions of neutral uranium<sup>12</sup>. The ground state hfs was studied by Childs et al.<sup>8</sup>. Upper-state hfs of transitions (purple lines) were studied by Avril et al.<sup>10</sup>. Hyperfine spectra of transitions (green lines) were obtained by Phillips et al.<sup>11</sup>. The blue line represents the transition studied here.

## Experimental

A schematic of our experimental setup for conducting SAS of uranium atomic beams is shown in Fig. 2.

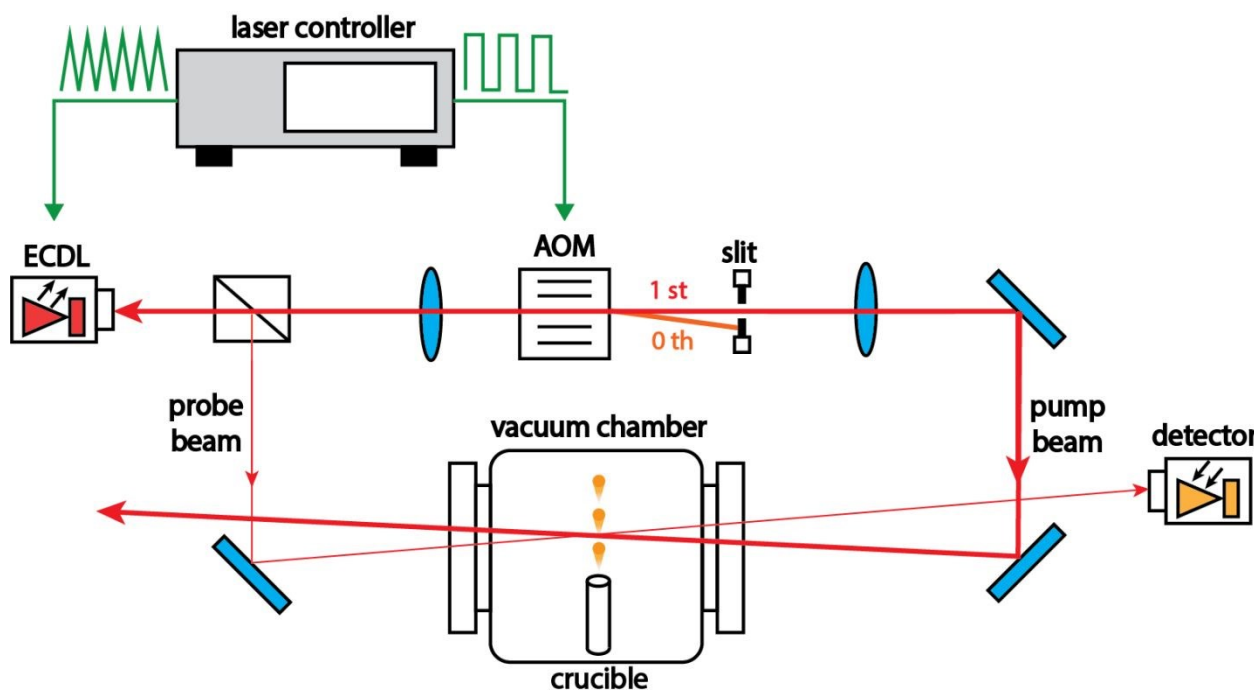


Fig. 2. Schematic of the saturation absorption spectroscopy experimental setup.

Our scheme for efficient generation of collimated atomic beams of uranium has been described previously<sup>6,7</sup>. The output from a narrow-band external-cavity diode laser (ECDL, Toptica Photonics, Germany) is divided by a 1:9 beam splitter into probe and pump beams. To obtain rapid extinction switching of the pump beam, an acousto-optic modulator (AOM, Brimrose Corp., USA) with a 35 ns rise time is used. The weaker probe beam ( $150 \mu\text{W}/\text{cm}^2$ ) was directed through the vacuum chamber in the counter propagating direction relative to the stronger pump beam (up to  $50 \text{ mW}/\text{cm}^2$ ) and detected by a silicon photodiode (Thorlabs, USA). The pump beam intersects with the probe beam right above the crucible and burns a spectral hole in the velocity profile of the uranium atoms. A 6 Hz sawtooth signal generated by the laser driver was employed to scan the ECDL frequency across a 15 GHz region centered around the 861.031 nm transition of uranium to observe both  $^{235}\text{U}$  and  $^{238}\text{U}$  absorption lines. Simultaneously, a 3 Hz AOM square signal was generated synchronously with the laser driver sawtooth signal, such that the pump beam was switched-off at a rate corresponding to every other round trip of the scan.

Three uranium samples of different  $^{235}\text{U}$  isotopic content were used in these studies. A natural uranium metal Standard Reference Material (SRM960, also known as CRM112A) containing 0.72017  $^{235}\text{U}$  atom percent, a locally sourced low-enriched metal uranium sample containing 19.879  $^{235}\text{U}$  atom percent, as determined by mass spectrometry, and a high-enriched uranium oxide Certified Reference Material (CRMU630) containing 63.353  $^{235}\text{U}$  atom percent.

**Uranium electronic structure.** The ground state of uranium has a total electronic angular momentum quantum number  $J = 6$ , while the upper state of the 861.031 nm transition has  $J = 5$ .  $^{235}\text{U}$  has a nuclear magnetic moment quantum number  $I = 7/2$ . As a result, there are twenty-one hyperfine transitions for  $^{235}\text{U}$  allowed by electric-dipole transition selection rules. These transitions are shown in Fig. 3. There are eight transitions in which the total angular momentum quantum number  $F$  decreases by one unit ( $F \rightarrow F - 1$ ), seven transitions where  $F$  remains the same ( $F \rightarrow F$ ) and six transitions where  $F$  increases by one unit ( $F \rightarrow F + 1$ ).

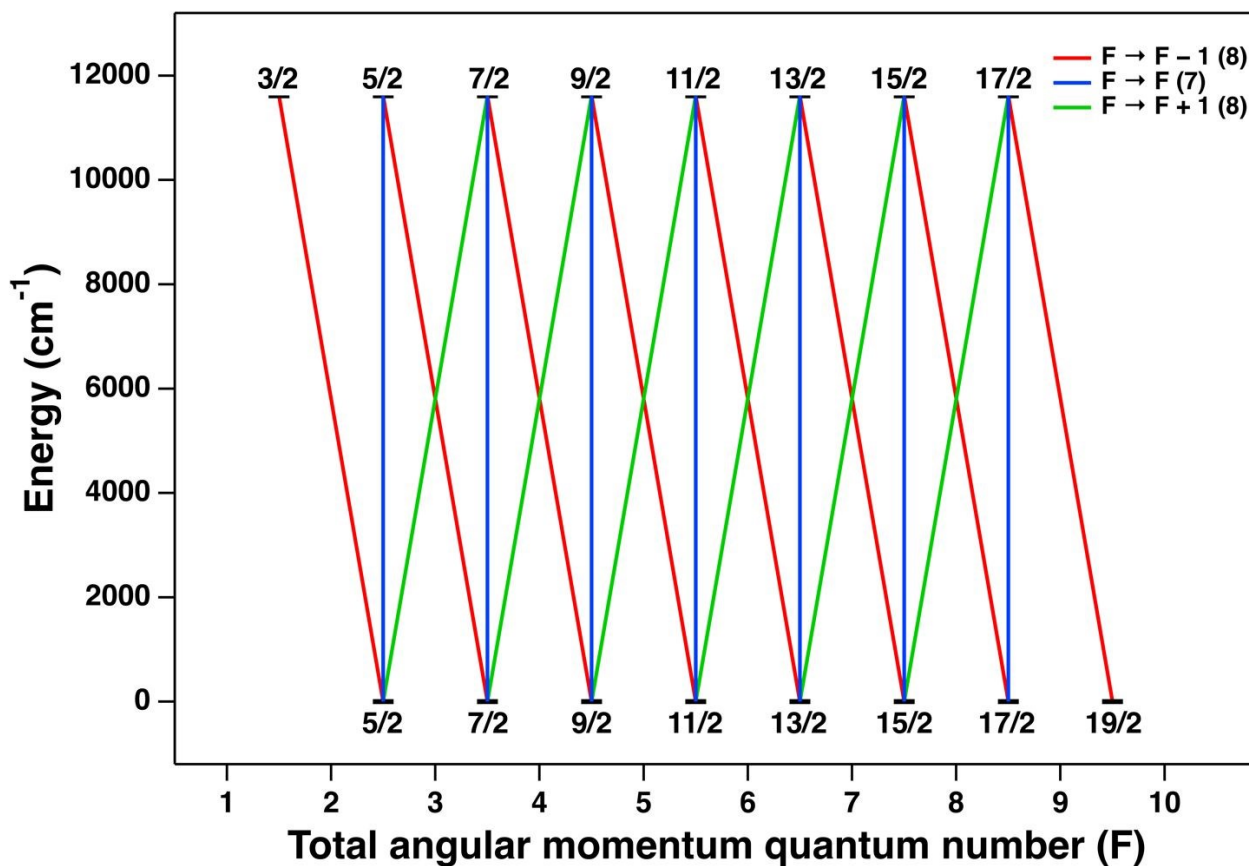


Fig. 3. Energy level diagram of the  $^{235}\text{U}$  transition at 861.031 nm. The numbers in parentheses indicate the number of transitions belonging to each category.

Though the number of hyperfine transitions for  $^{235}\text{U}$  is known, knowledge of relative line strengths and line energies is necessary for understanding the partially resolved  $^{235}\text{U}$  absorption spectrum. Based on the work of Axner *et al.*<sup>18</sup>, we calculated the relative hyperfine line strengths of  $^{235}\text{U}$  at 861.031 nm (Table 1). These line strengths can be normalized to the total intensity for the multiplet, which equals the single line strength for  $^{238}\text{U}$ .

**Table 1. Hyperfine structure of the 861.031 nm transition of  $^{235}\text{U}$**

|                 | $F_1$ | $E_1$ (cm $^{-1}$ ) | $F_2$ | $E_2$ (cm $^{-1}$ ) | $E_2 - E_1$ (cm $^{-1}$ ) | Relative strength |
|-----------------|-------|---------------------|-------|---------------------|---------------------------|-------------------|
| $\Delta F = -1$ | 5/2   | 0.1410              | 3/2   | 11613.9270          | 11613.7860                | 0.0455            |
|                 | 7/2   | 0.1106              | 5/2   | 11613.9139          | 11613.8032                | 0.0568            |
|                 | 9/2   | 0.0769              | 7/2   | 11613.8965          | 11613.8196                | 0.0714            |
|                 | 11/2  | 0.0438              | 9/2   | 11613.8760          | 11613.8322                | 0.0890            |
|                 | 13/2  | 0.0162              | 11/2  | 11613.8538          | 11613.8375                | 0.1097            |
|                 | 15/2  | 0.0000              | 13/2  | 11613.8314          | 11613.8314                | 0.1337            |
|                 | 17/2  | 0.0017              | 15/2  | 11613.8109          | 11613.8092                | 0.1612            |
|                 | 19/2  | 0.0290              | 17/2  | 11613.7946          | 11613.7656                | 0.1923            |
| $\Delta F = 0$  | 5/2   | 0.1410              | 5/2   | 11613.9139          | 11613.7729                | 0.0114            |
|                 | 7/2   | 0.1106              | 7/2   | 11613.8965          | 11613.7859                | 0.0186            |
|                 | 9/2   | 0.0769              | 9/2   | 11613.8760          | 11613.7991                | 0.0232            |
|                 | 11/2  | 0.0438              | 11/5  | 11613.8538          | 11613.8100                | 0.0250            |
|                 | 13/2  | 0.0162              | 13/2  | 11613.8314          | 11613.8152                | 0.0240            |
|                 | 15/2  | 0.0000              | 15/2  | 11613.8109          | 11613.8109                | 0.0197            |
|                 | 17/2  | 0.0017              | 17/2  | 11613.7946          | 11613.7928                | 0.0119            |
|                 | 5/2   | 0.1410              | 7/2   | 11613.8965          | 11613.7555                | 0.0009            |
| $\Delta F = +1$ | 7/2   | 0.1106              | 9/2   | 11613.8760          | 11613.7654                | 0.0015            |
|                 | 9/2   | 0.0769              | 11/2  | 11613.8538          | 11613.7769                | 0.0016            |
|                 | 11/2  | 0.0438              | 13/2  | 11613.8314          | 11613.7876                | 0.0013            |
|                 | 13/2  | 0.0162              | 15/2  | 11613.8109          | 11613.7947                | 0.0009            |

|                  |      |        |      |            |            |        |
|------------------|------|--------|------|------------|------------|--------|
|                  | 15/2 | 0.0000 | 17/2 | 11613.7946 | 11613.7946 | 0.0004 |
| <sup>238</sup> U | 0    | 0.0000 | 0    | 11613.9771 | 11631.9771 | 1.0000 |

The energies of the hyperfine transitions are calculated from differences between lower- and upper-state sublevels, while the hyperfine sublevel energies  $W_F$  of both lower and upper states can be calculated from the hyperfine magnetic-dipole constant  $A$  and electric-quadrupole constant  $B$  if higher orders of multipolar expansion can be neglected<sup>11</sup>:

$$W_F = A(C/2) + B[3C(C + 1) - 4IJ(I + 1)(J + 1)]/[8IJ(2J - 1)(2I - 1)],$$

where  $C$  is

$$C = F(F + 1) - I(I + 1) - J(J + 1).$$

The  $A = 2.0186 \pm 0.0001$  mK and  $B = 136.805 \pm 0.007$  mK values for the ground state were taken from Childs et al.<sup>9</sup>. We conducted SAS experiments to obtain the  $A$  and  $B$  values of the upper state. During the least-squares fitting process,  $A$  and  $B$  were floated, and the relative hyperfine transition intensities shown in Table 1 were fixed. Due to the fact that the number density of neutral uranium atoms cannot be precisely controlled during the generation of atomic beams, and the lack of knowledge about the absolute value of the 861.031 nm transition line strength, the amplitude of the fitted hyperfine transition lines was floated.

## Results and Discussion

Absorption scans with and without saturation were obtained from low-enriched uranium atomic beams generated from the 19% <sup>235</sup>U sample. Typical averages of 60 spectra are shown in Fig. 4a for each case. The difference on absorbance spectra obtained with and without pump results as a significant fraction of atoms were excited from the ground state to the excited state by the pump beam and are unable to absorb the probe beam, causing a dip in the spectrum. This difference has the largest amplitude when the laser is on

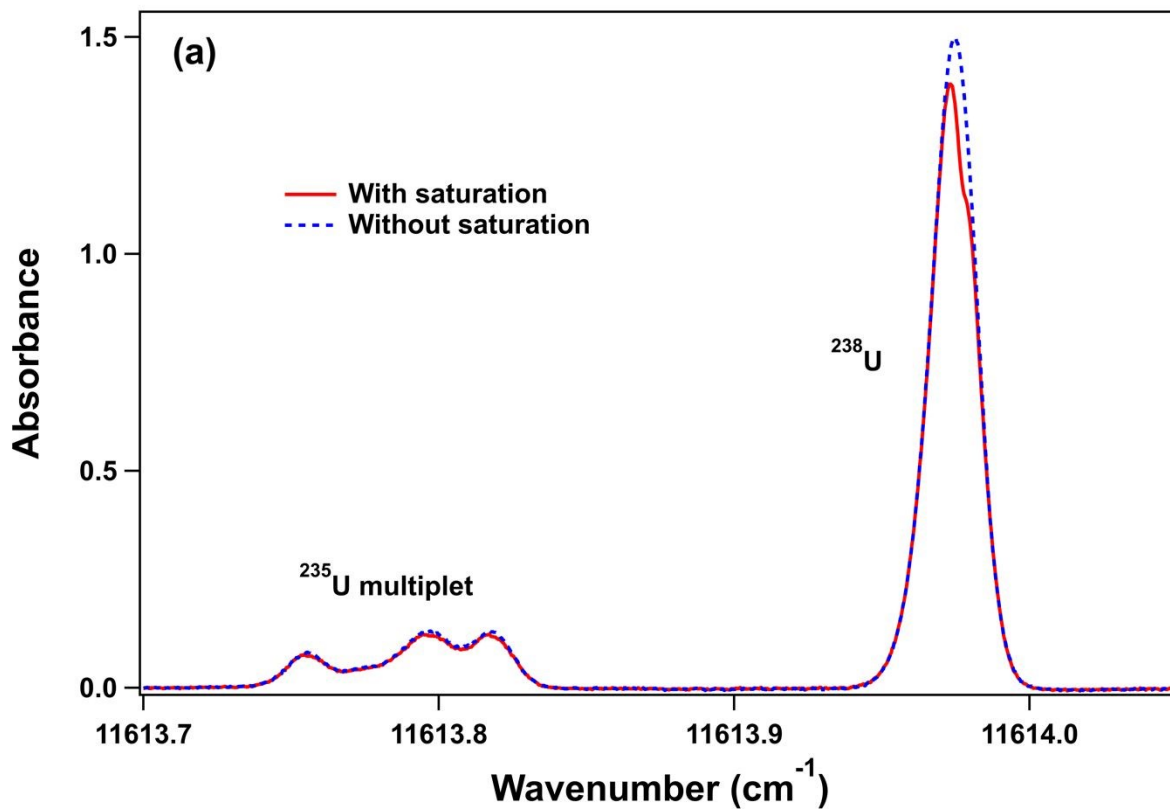
resonance. Fig. 4b shows the average of the differences between the absorbance spectra obtained with and without pump, in order to reveal the reduced Doppler-broadening hyperfine lines. The fitting process described above was used to obtain the magnetic-dipole (A) and electric-quadrupole (B) values which generated the best-fitted spectrum. The best-fit SAS spectrum is shown also in Fig. 4b. The fit captures most of the hfs details, while small discrepancies are caused by neglected higher-orders multipolar expansion terms and measurement errors, as expected. The relative line strengths of the hyperfine transitions are shown also in Fig. 4b. The initial and final total angular momentum numbers of the top four strongest transitions along with the  $5/2 \rightarrow 3/2$  transition are labeled in Fig. 4b. This measurement was repeated five times, and the obtained average values for the hfs constants A and B are:

$$A = -3.2887 \pm 0.1957 \text{ mK},$$

$$B = 31.8712 \pm 8.0789 \text{ mK}.$$

**Theoretical Calculations.** In conjunction with the experimental measurements and fittings, we have performed relativistic configuration-interaction (RCI) electronic structure calculations of the magnetic dipole A and electric quadrupole B for comparison<sup>19</sup>. The method was tested on previously measured values of hyperfine constants of U I, and good agreement was observed. It has been found that the agreement with previous measurements can be improved by multiplying the A values of hyperfine constant obtained with RCI method (the “vse” basis in which the excitations over the principal quantum numbers are saturated) by a factor of 1.124. The specific even level we consider in the current work has uncertainty with respect to which configuration has to be chosen. If we assume  $5f^37s^27p$ , which is consistent with the Cotton database<sup>20</sup>, then  $A_{th} = -3.487 \text{ mK}$ , or if we assume  $5f^26d^27s^2$  [19,20],  $A_{th} = -2.979$ . The agreement is better in the case of the  $5f^37s^27p$  configuration. The electric quadrupole hyperfine constants are:  $B_{th} = 73.69 \text{ mK}$  and  $145.81 \text{ mK}$ , in the case of  $5f^37s^27p$  and  $5f^26d^27s^2$  configurations, respectively. The agreement of the experimental B constant with the first value is better. It is possible that the two configurations are mixed, with dominance of the  $5f^37s^27p$  configuration. The theoretical calculations yield a substantial error bar for B (about 30 mK) due to the sensitivity to the choice of the

1  
2  
3 configuration and other calculation parameters. The experimental g factor 0.740 is  
4 closer to the theoretical value of 0.7423 (assuming  $5f^37s^27p$ ) rather than 0.7361  
5 (assuming  $5f^26d^27s^2$ ), both calculated with the same RCI vse method.  
6  
7



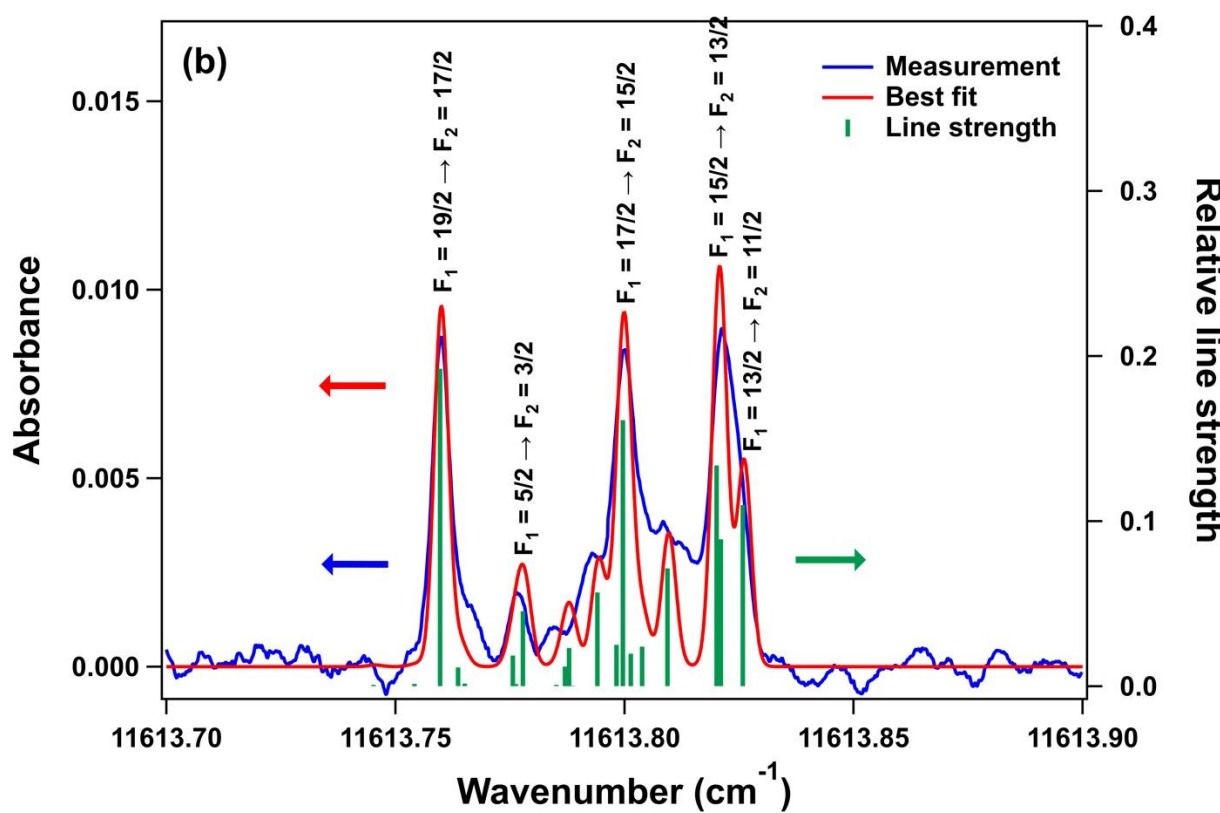


Fig. 4. (a) SAS spectrum of uranium at 861.031 nm with and without saturation. The inset highlights the spectrum details of the  $^{235}\text{U}$  isotope. (b) Average of measured Doppler-free spectra and best-fit. The relative line strengths of hyperfine transitions are shown as green bars.

With the knowledge of the  $^{235}\text{U}$  hfs, a uranium isotope-ratio determination strategy can be optimized based on the required precision, and also on the specific spectroscopic measurement being employed. Theoretically, the more hyperfine transitions that are used for spectrum fitting, the smaller is the fitting residual obtained, and the higher precision can be achieved. However, under certain circumstances, the use of an increasing number of transitions does not necessarily result in an improved fitting result. For instance, when the measurement is dominated by noise in a harsh environment, the inclusion of hyperfine transitions with small line strengths does not improve the measurement precision. We compared the fitted spectra and obtained isotopic ratios for several strategies which utilized a different number of hyperfine transitions. A  $\text{U}_3\text{O}_8$  Certified Reference Material containing 63.353%  $^{235}\text{U}$  (U630) was used for these experiments. Atomic beams of neutral (non-ionized) uranium were generated following a previously described chemical

1  
2  
3 reduction scheme that uses lutetium to reduce the oxide<sup>6</sup>. During the spectral fitting  
4 process, the positions and relative line strengths were fixed for the selected hyperfine  
5 transitions, while the total amplitude and widths were floated. A Voigt line shape model  
6 was used in order to include the broadening effects brought by imperfect atomic beam  
7 collimation and a small angle between the pump and probe laser beams, and the same  
8 width values were given to all hyperfine transitions.  
9  
10

11 Fig. 5a shows a comparison between a typical measured spectrum and the best-fitted  
12 spectrum which utilized the four strongest hyperfine transitions. It can be seen that the  
13 three strongest peaks of the absorption spectrum located at 11613.76 cm<sup>-1</sup>, 11613.80  
14 cm<sup>-1</sup> and 11613.83 cm<sup>-1</sup> were basically captured, while some noticeable discrepancies  
15 were observed, especially for the small peak located at 11613.78 cm<sup>-1</sup>, due to an  
16 insufficient number of spectral lines included in the fitting process. The standard deviation  
17 of the residual was calculated to be 0.12 (6.4% relative to the absorption amplitude). By  
18 contrast, Fig. 5b shows a comparison between a typical measured spectrum and the best-  
19 fitted spectrum which utilized all of the twenty-one hyperfine transitions. All of the details  
20 of the absorption spectrum were captured in this case, and an extremely small fitting  
21 residual was obtained, with a standard deviation of 0.008 (0.44% relative to the absorption  
22 amplitude). Additionally, fittings that included 7, 8, 11 and 15 hyperfine transitions were  
23 performed as well, and Fig. 6 shows the summary of the residual standard deviations for  
24 all of the fittings.  
25  
26  
27  
28  
29  
30  
31  
32  
33  
34  
35  
36  
37  
38  
39  
40  
41  
42  
43  
44  
45  
46  
47  
48  
49  
50  
51  
52  
53  
54  
55  
56  
57  
58  
59  
60

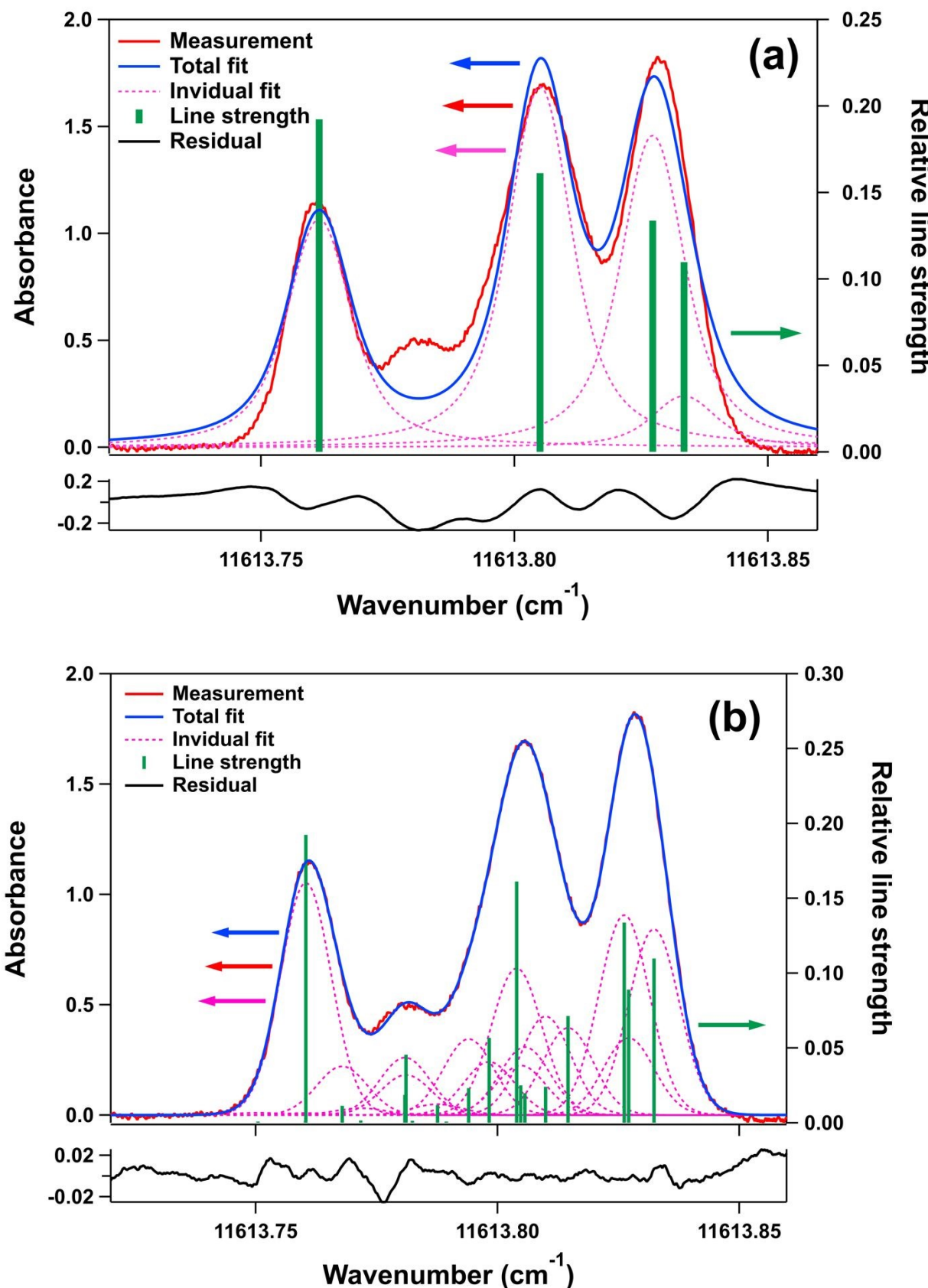


Fig. 5. (a) Comparison between the measured spectrum and a best-fitted spectrum which included four hyperfine transitions. (b) Comparison between the measured spectrum and a best-fitted spectrum which utilized 21 hyperfine transitions.

Fig. 6 also shows the  $^{235}\text{U}$  isotope ratios inferred from the integrated areas of the  $^{235}\text{U}$  and  $^{238}\text{U}$  peaks in the fitted spectra. The goodness of fit and precision are improved by increasing the number of hyperfine transitions. However, when the number of transitions included in the fit increases to 15 or more, the precision ceases to improve. This is due to the fact that the strengths of the  $\Delta F = +1$  transitions are small (see Table 1), and they have a minimal influence on the goodness of fit. We can conclude that, in this particular case, all of the hyperfine transitions with  $\Delta F = -1$  and  $\Delta F = 0$  should be utilized to obtain isotope ratios.

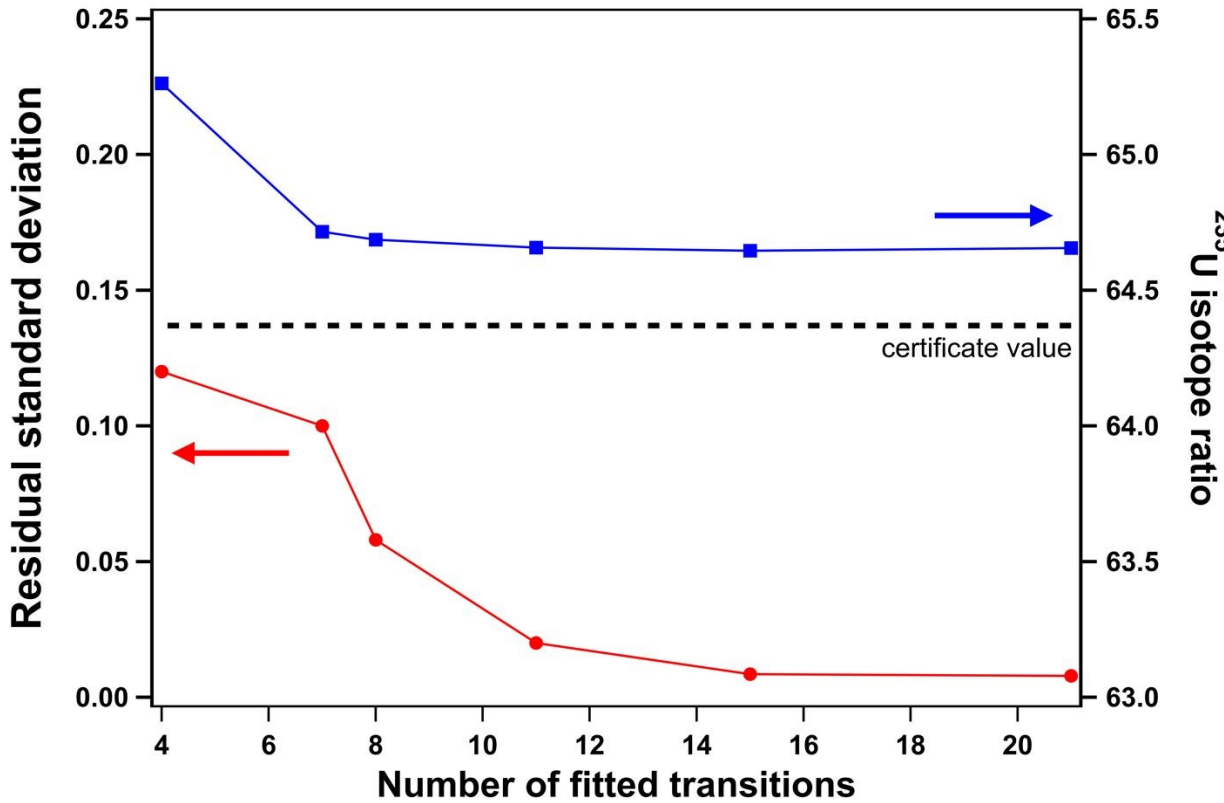


Fig. 6. The relationship between residual standard deviation, measured  $^{235}\text{U}$  isotope ratio, and the number of hyperfine transitions included in the fitting. The nominal  $^{235}\text{U}$  isotope ratio is shown as a green dashed line.

Finally, to be able to obtain a complete understanding of the 861.031 nm transition of uranium, we attempted to derive the absolute line strength from the SAS profile. When the width of the absorption profile is dominated by the natural linewidth, it can be used to determine the absolute line strength, as in the method described by McClelland<sup>23</sup>. In our SAS measurement, however, some additional broadening mechanisms were observed to contribute to the total width, and we analyzed them in order to extract the radiative linewidth. To minimize interferences from adjacent <sup>235</sup>U lines, measurements of the linewidth were carried out on the <sup>238</sup>U transition using natural uranium metal samples, which contain only 0.7% <sup>235</sup>U. SAS measurements were conducted at five different pump beam intensities, ranging from 2.8 to 25.7 mW·m<sup>-2</sup>. By assuming a Lorentzian profile and power broadening, the Lamb dip width  $\gamma$  (when the pump and probe originate from the same laser and are scanned simultaneously) is given by<sup>24</sup>:

$$\gamma = \gamma_0 \left(1 + \sqrt{1 + \frac{I}{I_{sat}}}\right)/2$$

where  $\gamma_0$  is the total Lorentzian width without saturation,  $I_{sat}$  is saturation intensity. Based on the RCI theory, the oscillator strength is calculated to be  $f = 0.1$  for our specific transition, which yields a natural width of  $\gamma_{nat} = 1.7$  MHz. In addition to natural broadening, self-collisional broadening is considered to contribute to the total Lorentzian width  $\gamma_0$  as well. The self-broadening can be estimated approximately using the equation given by Lewis<sup>25</sup>:

$$\gamma_{self} = N\beta_{self}$$

where  $N$  is number density,  $\beta_{self}$  is the self-broadening parameter given by:

$$\beta_{self} = 2fcr_0\lambda\sqrt{g_g/g_e}$$

where  $c$  is the speed of light,  $r_0$  is the classical radius of the electron,  $\lambda$  is transition wavelength, and  $g_g$  and  $g_e$  are the degeneracies of the ground and excited states, respectively. This equation was previously applied to alkali-metal atoms<sup>26</sup>, with close agreement found between measured and predicted self-broadening values. Based on the vapor pressure of neutral uranium at a temperature of 2200 °C, the number density is estimated to be  $N = 1.8 \times 10^{14}$  cm<sup>-3</sup>. Then, the self-broadening width is calculated to be

$\gamma_{\text{self}} = 4.5$  MHz, which, together with the natural width, gives the total Lorentzian width  $\gamma_0 = 6.2$  MHz. It can be seen that the width due to self-broadening may exceed the natural width, and it has to be included in the analysis for atomic densities exceeding  $10^{13}$  cm<sup>-3</sup>.

To minimize interferences from adjacent <sup>235</sup>U lines, measurements of the linewidth were carried out on the <sup>238</sup>U transition using natural uranium metal samples, which contain only 0.72% <sup>235</sup>U. By fitting the experimental data to Voigt profiles, we obtained the dependency of the Lorentzian width on the pump intensity, as shown in Fig. 7. It is worth mentioning that since there is a small angle between the pump and probe beam in the SAS measurement, there is residual Doppler broadening, and Voigt profiles should be used to extract the Lorentzian components. The Lorentzian width at zero intensity is extrapolated to be  $14.5 \pm 8.2$  MHz using the power-dependent Lorentzian width equation mentioned before. It is also possible that the RCI theory yields a low  $f$  value. If  $f$  is increased to 0.2 and 0.3, the total Lorentzian width  $\gamma_0$  is calculated to be 12.4 MHz and 18.6 MHz, respectively. Considering the uncertainties present in the experimental measurements, we estimate that  $f = 0.1$  to 0.3, which corresponds to  $A = 1$  to  $3 \times 10^7$  s<sup>-1</sup>.

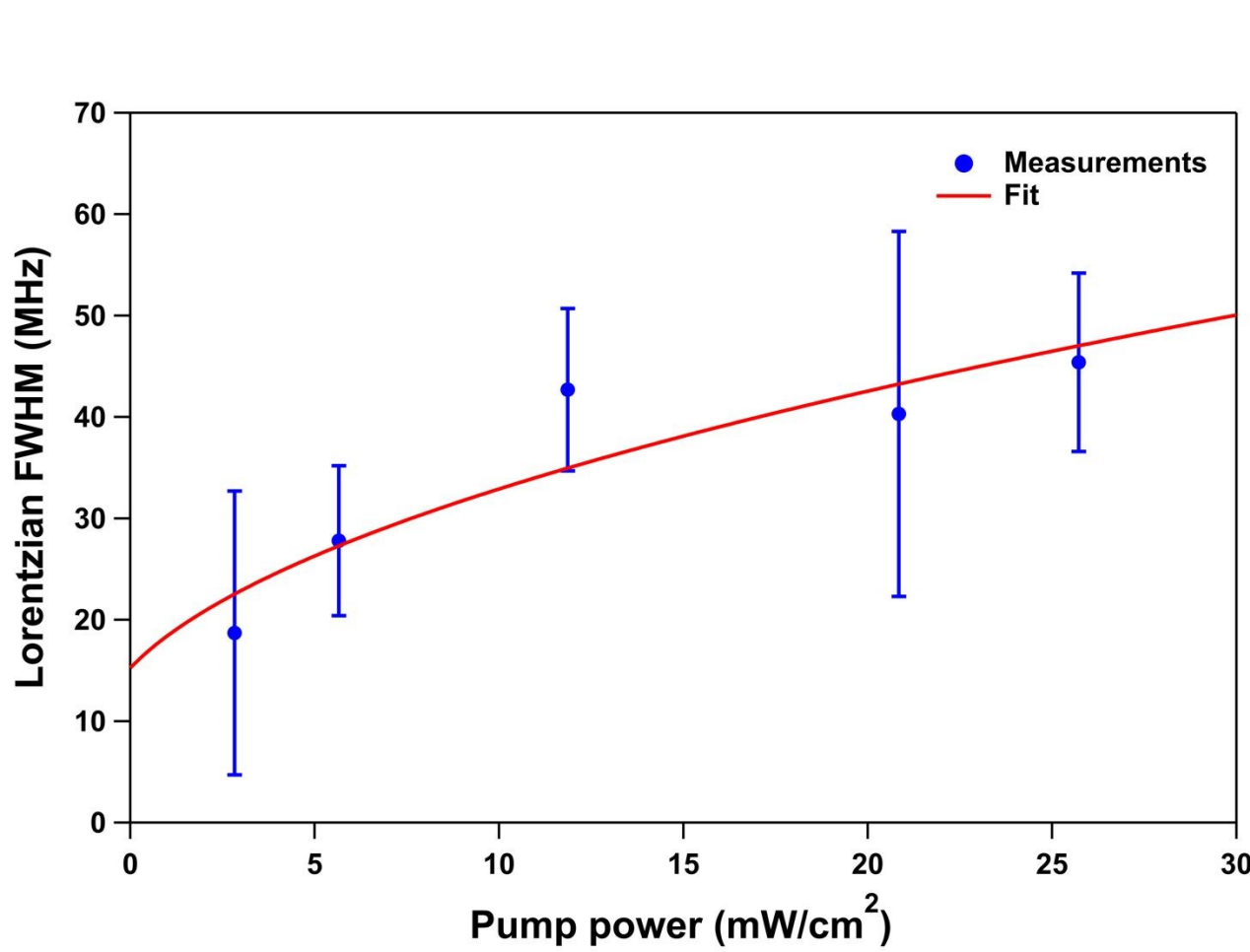


Fig. 7. Dependence of the Lorentzian width on pump power. The unsaturated Lorentz width is estimated to be  $14.5 \pm 8.2$  MHz.

## Conclusions

The 861.031 nm line has proven to be one of the most suitable transitions as the basis for the development of techniques for the isotopic analysis of uranium by laser absorption spectroscopy, due to the fact that this is the strongest transition from the ground state. We have employed SAS to study the hfs of the  $^{235}\text{U}$  isotope, taking advantage of potentially Doppler-free absorption spectroscopy using a combination of narrow-band, tunable diode lasers, a recently developed technique for efficient atomic beam generation, and rapidly switchable AOM. By applying normalized line strength values and fitting the simulated spectrum to the measured spectrum, the magnetic-dipole A and electric-quadrupole B constants, as well as the energies of the  $^{235}\text{U}$  hyperfine transitions,

were obtained. These constants were calculated using RCI theory and good agreement was found, especially in case of the A constant. This allows assigning the  $5f^37s^27p$  configuration to the upper state, instead of the previously reported  $5f^26d^27s^2$  configuration<sup>19</sup>. Additionally, we have demonstrated that the obtained information of  $^{235}\text{U}$  hyperfine transitions allows us to conduct accurate uranium isotope-ratio measurements in solid samples, and that the detection strategy can be optimized based on the requirements of our particular technique, and on the desired measurement precision. Finally, our SAS experimental line profiles were theoretically modeled to check the consistency of the RCI  $^{238}\text{U}$  oscillator strength and transition probability values with experimental observations. By comparing the fitted unsaturated Lorentzian width with the theoretical value, we estimate that the oscillator strength of this transition ranges from 0.1 to 0.3, which corresponds to an Einstein A coefficient range from  $1 \times 10^7 \text{ s}^{-1}$  to  $3 \times 10^7 \text{ s}^{-1}$ . This is a rough estimate, and more elaborated analysis and additional measurements are required to improve the precision.

## Conflicts of interest

There are no conflicts to declare.

## Acknowledgements

Parts of this work were supported by the ASC PEM program of the US Department of Energy through the Los Alamos National Laboratory and by US Department of State under IAA 193AVC20Y0006.

Los Alamos National Laboratory is operated by Triad National Security, LLC, for the National Nuclear Security Administration of U.S. Department of Energy (Contract No.9233218NCA000001).

## References

[1] S. Boulyga, S. Konegger-Kappel, S. Richter, and L. Sangély, *J. Anal. At. Spectrom.*, 2015, **30**, 1469–1489.

[2] F. E. Stanley, *J. Anal. At. Spectrom.*, 2012, **27**, 1821–1830.

[3] M. Wallenius, K. Mayer, and I. Ray, *Forensic Sci. Int.*, 2006, **156**, 55-61.

[4] A. D. Pollington, W. S. Kinman, S. K. Hanson, and R. E. Steiner, *J. Radioanal. Nucl. Chem.*, 2016, **307**, 2109–2115.

[5] V. Lebedev, J. H. Bartlett, A. Malyzhenkov, and A. Castro, *Rev. Sci. Instrum.*, 2017, **88**, 126101.

[6] V. Lebedev, J. H. Bartlett, and A. Castro, *J. Anal. At. Spectrom.*, 2018, **33**, 1862–1866.

[7] J. H. Bartlett and A. Castro, *Spectrochim. Acta B*, 2019, **155**, 61–66.

[8] S. Gerstenkorn, P. Luc, Cl. Bauche-Arnoult, and D. Merle, *J. Phys. (Paris)*, 1973, **34**, 805–812.

[9] W. J. Childs, O. Poulsen, and L. S. Goodman, *Opt. Lett.*, 1979, **4**, 35–37.

[10] W. J. Childs, O. Poulsen, and L. S. Goodman, *Opt. Lett.*, 1979, **4**, 63–65.

[11] R. Avril, A. Ginibre, and A. Petit, *Z. Phys. D*, 1994, **29**, 91–102.

[12] M. C. Phillips, B. E. Brumfield, N. Lahaye, S. S. Harilal, K. C. Hartig, and I. Jovanovic, *Sci. Rep.*, 2017, **7**, 3784.

[13] N. R. Taylor, and M. C. Phillips, *Opt. Lett.*, 2014, **39**, 594-597.

[14] B. A. Palmer, R. A. Keller, and R. Engleman, "Atlas of uranium emission intensities in a hollow cathode discharge," Los Alamos National Laboratory report LA-8251-MS, Los Alamos, N.M., 1980.

[15] G. R. Hanes, J. Lapierre, P. R. Bunker, and K. C. Shotton, *J. Mol. Spectrosc.*, 1971, **39**, 506–515.

[16] P. Kumar, V. K. Saini, G. S. Purbia, Om Prakash, S. K. Dixit, and S. V. Nakhe, *Appl. Opt.*, 2017, **56**, 1579–1584.

[17] Y. Huang, Y. Guan, T. Suen, J. Shy, and L. Wang, *Appl. Opt.*, 2018, **57**, 2102–2106.

[18] O. Axner, J. Gustafsson, N. Omenetto, J. D. Winefordner, *Spectrochim. Acta B*, 2004, **59**, 1–39.

[19] I. M. Savukov, *Phys. Rev. A*, 2020, **102**, 042806.

[20] Laboratoire Aimé Cotton atomic structure database: <http://www.lac.u-psud.fr/old-lac/lac/Database/Tab-energy/Uranium/U-tables/U1e-1.html>.

[21] J. Blaise and L. J. Radziemski, *J. Opt. Soc. Am.*, 1976, **66**, 644–659.

[22] Z. B. Osman, *Contribution à la classification des spectres d'arc et d'étincelle de l'uranium par l'étude des structures zeeman entre 4700 et 3100 Å et du déplacement isotopique*, Université de Paris Docteur Thesis, 1966.

[23] J. J. McClelland, *Phys. Rev. A*, 2006, **73**, 064502.

[24] W. Demtröder, *Laser Spectroscopy 2: Experimental Techniques*, Fifth Edition, Springer, Berlin, p. 99, 2015.

[25] E. L. Lewis, *Phys. Rep.*, 1980, **58**, 1–71.

[26] L. Weller, R. J. Bettles, P. Siddons, C. S. Adams and I. G. Hughes, *J. Phys. B: At. Mol. Opt. Phys.*, 2011, **44**, 195006.